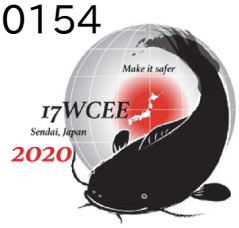

17th World Conference on Earthquake Engineering, 17WCEE
Sendai, Japan - September 13th to 18th 2020

STUDY ON FATIGUE BEHAVIOR OF TIMBER SHEAR WALLS SUBJECTED TO REPEATED CYCLIC LOADING

Y. Yamazaki [(1)], K. Kanda [(2)], H. Sakata [(3)]

[(1)] *Senior research engineer, Building Research Institute, y_ymzk@kenken.go.jp*
[(2)] *Former graduate student, Tokyo Institute of Technology, kanda.k.ac@m.titech.ac.jp*
[(3)] *Professor, Tokyo Institute of Technology, sakata.h.aa@m.titech.ac.jp*

Abstract

Conventional test program for timber shear walls in Japan uses a loading protocol consisting of monotonic loading following reverse cyclic loading up to 1/50rad. While repeated cyclic loading is thought to decrease force and deformation capacity due to the fatigue behavior, specimens tested by the conventional program might not sustain damage at large deformation range. Although timber shear walls had better have large deformation capacity, it is not always empirically confirmed. Recently, buildings are required to protect not only the safety but the property after a major earthquake, and passive control techniques for timber structures have been developed in order to enhance the seismic performance. Therefore, evaluation of timber shear walls' fatigue behavior have become an important issue.

In this study, evaluation of strength and energy dissipation of two typical timber shear walls subjected to various deformation history is dealt with. Static loading tests and shaking table tests are conducted. Finally, evaluation formulae for strength and equivalent damping ratio is proposed. The followings are findings of this paper.

1) Envelope curve of force-deformation angle relation has dependency on loading protocol. The envelope curve in monotonic loading is the upper limit, and the others go down as the number of cycles becomes large.

2) Plywood type shear walls are vulnerable to repeated loading rather than brace type shear walls, which is likely to be related to the failure mode. As for plywood type shear walls, when small number of cycles was applied, failure mode of nail joint was punching out. However, when large number of cycles was applied, nail joint was fractured by bending.

3) Evaluation formulae for strength and equivalent damping ratio considering fatigue behavior were proposed. The formula for strength has a unique parameter controlling damage effect when the deformation amplitude is expanded. The formula for equivalent damping ratio is empirically derived based on the fact that equivalent damping ratio has strong dependency on the already experienced maximum deformation rather than the number of cycles. They showed acceptable agreement with results of static random loading tests and shaking table tests.

Keywords: timber brace wall, plywood sheathing wall, performance deterioration, accumulated damage

1. Introduction

Conventional test program for timber shear walls in Japan uses a loading protocol which consists of monotonic loading following progressive increasing reverse cyclic loading up to 1/50rad[1]. While repeated cyclic loading is thought to decrease the force and deformation capacity due to the fatigue behavior, specimens tested by the conventional test program might not sustain enough cycles at large deformation range. Although timber shear walls had better have large deformation capacity, it might not be always empirically confirmed. Recently, buildings are required to protect not only the safety but the property after a major earthquake, and passive control techniques for timber structures have been developed in order to enhance the seismic performance and the post-earthquake functional use. Therefore, evaluation of timber shear walls' fatigue behavior has become an important issue[2-4].
Several experiment-based studies on timber shear walls' fatigue behavior can be found[5-10], and some of them have proposed hysteresis model for time history analysis. CUREE model is one of the most frequently

used hysteresis model for wooden structures[5], and EPHM model is also well-known model preciselly tracing the deterioration behavior[6]. Japanese researchers often refer to them, and the modified models have been proposed[7-10]. However, time history analysis is rarely used for seismic design of timber detached houses owing to the cost of time and effort. In many cases, simplified design methods like allowable design method or response spectrum method are utilized, and they require basic characteristics like envelope curve of base shear force-story drift angle relation and equivalent damping ratio instead of hysteresis model.
In this study, strength and energy dissipation of two typical timber shear walls subjected to repeated cyclic loading are focused on. Static loading tests and shaking table tests are introduced. Finally, evaluation formulae for strength and equivalent damping ratio are proposed [11].

2. Static loading test with various loading protocol

2.1 Specimens and test setup

Specimens and test setup are shown in Fig.1 and Fig.2, respectively. Dimensions and material properties of members are summarized in Table1. Two types of specimens, "Brace type(B)" and "Plywood type(P)", were tested.

Brace type has 1820mm length(post span = 910mm) and inverse V-shape braces. The dimension of braces is 45mm x 60mm. Gypsum boards(t=12.5mm) are fastened by nails on posts and studs. Box shape gusset plates are attached to braces' connections.

Plywood type has 910mm length. Plywood(t=9mm) is fastened by nails on posts and beams.

Both types have hold down in the bottom and top ends of posts. 5kN of initial tension was applied to anchor bolts of hold down. Ground sill was fixed on the steel beam, and lateral force was applied to the top beam by the actuator. Shear deformation angle δ was controlled.

Table1 Specification of members

Member	Tree species	Cross sect. (mm)	Grade	Moisture cont. (%)	Specific gravity	MOR (N/mm^2)	MOE (kN/mm^2)
Beam	Scotch pine Symmetric const.	105x180	E105-F300	7.1 10	0.50	67.5	13.2
Ground sill	Scotch pine Homogeneous const.	105x105	E95-F315	7.1 10.4	0.47	43.8	10.7
Post	Spruce Homogeneous const.	105x105	E95-F315	6.7 10.3	0.46 0.45	45.3	12.4 12.1
Brace	Western hemlock	45x90	E120	8.1 11.6	0.45 0.47	67.5 90.8	9.6 12.4
Stud	White	105x45	-	6.9 11.0	0.47	-	-

Member	Type	Dimension (mm)	Thickness (mm)	Connection			Moisture cont. (%)
				Nail	Pitch (mm)	Edge dist.(mm)	
Gypsum board	GB-R	910x2420	12.5	GN40	150	10	-
Plywood	Structural plywood Softwood	910x2730	9	N50	150	V:15, H:12	7.0

Upper: chapter2, Lower: chapter3

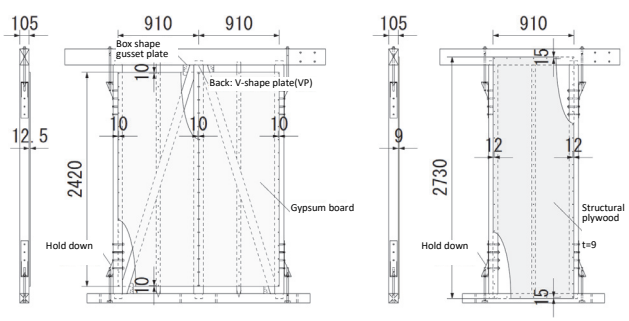

(a) Brace type (b) Plywood type

Fig.1 Front/side view of specimens

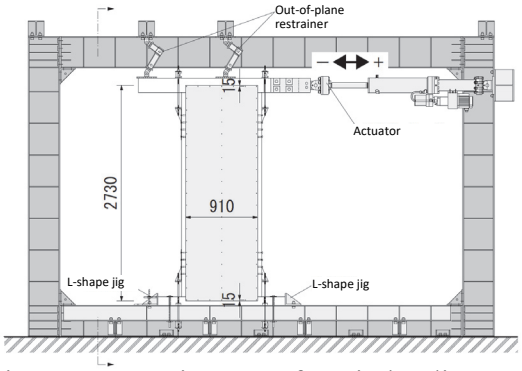

Fig.2 Test equipment of static loading test

2.2 Loading protocols

Four types of loading protocols were applied as shown in Fig.3.

"Standard loading" is described in the design standard[1] (Fig.3(a)). Monotonic loading is applied following reverse cyclic loading: three cycles in δ = 1/450, 1/300, 1/200, 1/150, 1/100, 1/75, 1/50 rad and one cycle in 1/30 rad. The monotonic loading was stopped at the ultimate deformation angle δ_u which is defined as the deformation angle when the corresponding force comes down up to 80% of P_{max}.

"Monotonic loading" is just pushover up to ultimate deformation angle δ_u (Fig.3(b)).

"Constant amplitude loading" consists of thirty cycles in ultimate deformation angle δ_u after thirty cycles in $\delta_u\Delta$ (Fig.3(c)). Where, Δ is a multiplier named "amplitude ratio", which is not larger than 1. Δ = 1, 2/3, 1/2, 1/4 are considered, and Δ = 1/3 is added in the case of plywood type.

"Random loading" considers earthquake responses simulated by single degree of freedom system modeled in reference[3] (Fig.3(d),(e)). Triangular wave with low velocity was applied as static random loading. Various input motions were tried, and Fukiai N240E and JMA Kobe NS, the 1995 Hyogoken-nambu earthquake were chosen, each of which was named "long duration wave" and "short duration wave", respectively.

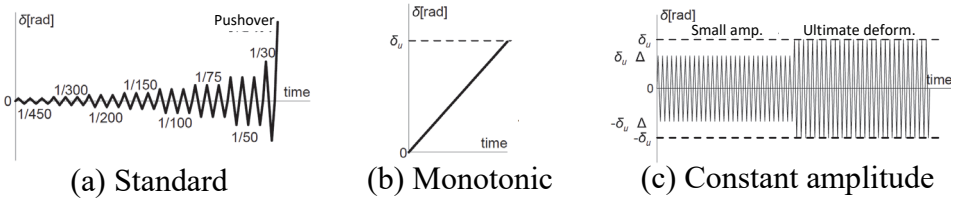

(a) Standard (b) Monotonic (c) Constant amplitude

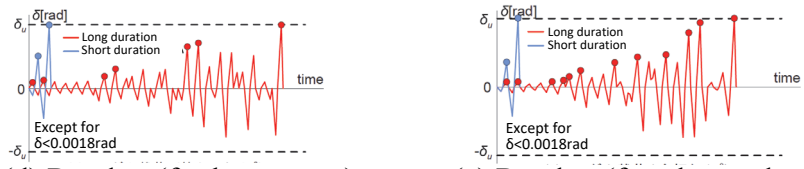

(d) Random(for brace type) (e) Random(for plywood type)

Fig.3 History of deformation angle

2.3 Force-deformation angle relation

Envelope curves of force-deformation angle relation are shown in Fig.4 with respect to each loading protocol. The averaged curve of monotonic loadings is named "standard envelope(Std. env.)"(Fig.4(a)), and δ_u is defined according to this curve.

In the case of constant amplitude loading(Fig.4(b)), smaller Δ gave little damage and strength degradation while larger Δ had a large effect in the envelope curve. The maximum force of plywood types was

significantly decreased compared to standard envelope(bold dash line) when Δ larger than 1/3 was applied. Plywood type was likely to be more vulnerable to repeated cyclic loading.

In the case of standard loading and random loadings(Fig.4(c)), strength degradation was observed to a greater or lesser extent. Standard loading gave the largest strength degradation in brace type while long duration wave had the largest impact in plywood type.

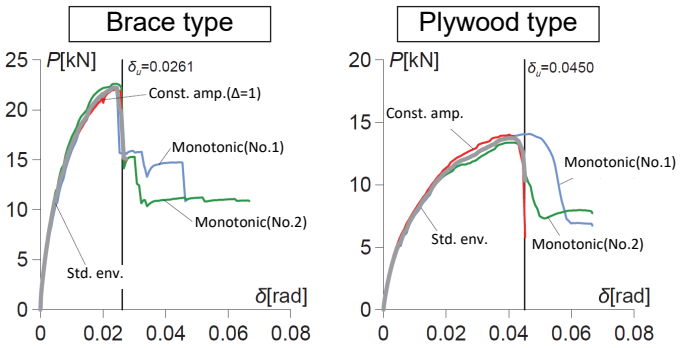

(a) Monotonic loading

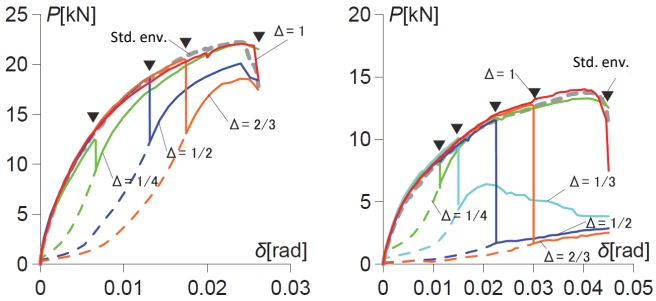

(b) Constant amplitude loading

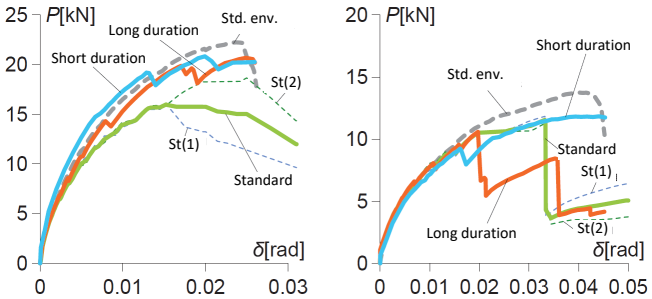

(c) Standard/Rrandom loading

Fig.4 Comparison of envelope curves with respect to each loading protocol

2.4 Tendency of strength deterioration

The tendency of strength degradation in constant amplitude loading is discussed. Force at cycle number n is normalized by the one of the standard envelope at the corresponding deformation, and the tendency along n is defined as $f(\Delta, n)$ meaning strength reduction ratio. n is the already experienced cycle number.

$f(\Delta, n)$ is shown in Fig.5 with respect to each Δ. $f(\Delta, n)$ approaches a lower limit and is gradually stabilized like an exponential function. As Δ becomes large, the lower limit decreases and the velocity of convergence becomes more rapidly. In the case of plywood type, the tendency is likely to be more significant, and it corresponds to previous researches[10].

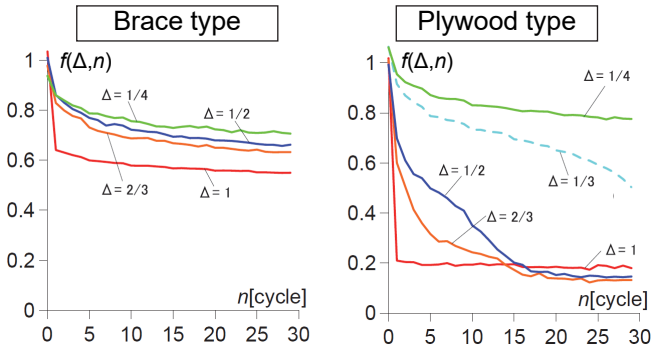

Fig.5 Strength deterioration when subjected to constant amplitude loading

2.5 Failure mode

In the case of brace type, typical failure modes were fracture in brace connection subjected to tensile force(Fig.6(a)), buckling of brace and crack of gypsum board(Fig.6(b)). Gypsum board was fractured around nail joints, and then it was pushed by the buckled brace resulting in crack or dropping. Loading protocols not including small deformation cycles like monotonic tended to show dropping of gypsum board without cracks. Even though failure modes of gypsum board were clearly affected by loading protocols, strength degradation of brace type had less dependency on loading protocols as well as bare braces[10].

In the case of plywood type, typical failure modes were punching out and bending fracture of nails(Fig.7(a),(b)). The number of nails fractured by bending is shown in Fig.8 with respect to each loading protocol. The number was counted after the test. Medium amplitude of cycles like Δ = 2/3, 1/2 and 1/3 was likely to cause more bending fractures because the cycles firstly triggered pullouts of nails which decreases the possibility of punching out(Fig.7(c)). Monotonic-like loading brought more punching out rather than bending fractures. Note that the tendency of standard loading was more similar to monotonic one. Small amplitude of cycles like Δ = 1/4 caused less bending fractures, which was concentrated on upper and lower rows of nails.

(a) Tensile fracture of brace connection (b) Crack of gypsum board

Fig.6 Observed failure mode of brace type wall

(a) Punching out (b) Bending fracture (c) Pullout

Fig.7 Observed failure mode of plywood type wall (nail joints)

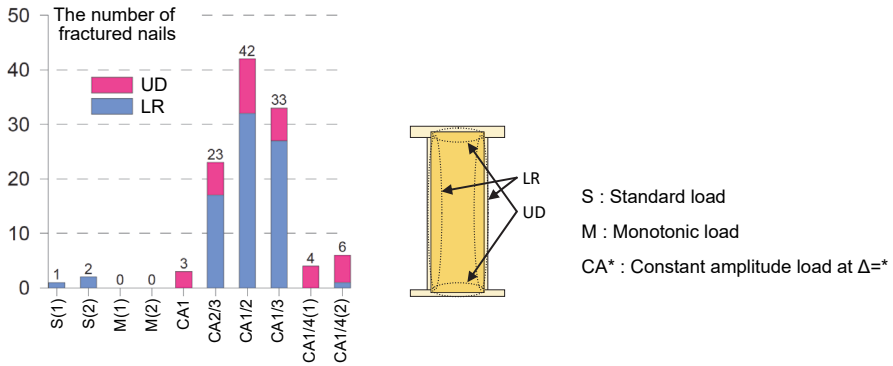

Fig.8 The number of fractured nails(Plywood type)

3. Shaking table test

3.1 Specimens

Specimens and test setup are illustrated in Fig.9 and Fig.10, respectively. Dimension and material properties of members are shown in Table1. Uni-axial input motion was applied to the specimens. The specimens have the same walls as the ones tested in the last chapter. Additional mass was put on the roof, and the weight was determined so that the specimens would have design base shear coefficient C_0 = 0.2(Seismic grade1) or 0.3(Seismic grade3). C_0 can be calculated as allowable strength divided by the weight by referring to the test results in the last chapter. Two types of walls(B, P) and two levels of seismic grade(1, 3) were considered, and the total four specimens named "B1", "B3", "P1" and "P3" were simultaneously shaken.

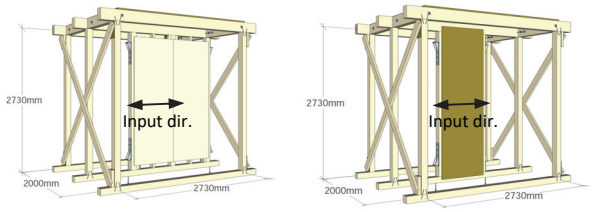

(a) Brace type (b) Plywood type

Fig.9 Single-story specimens

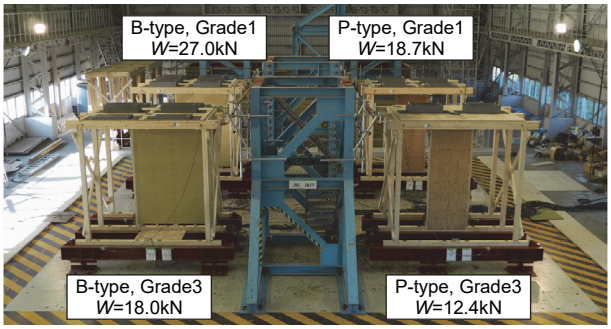

Fig.10 Shaking table

3.2 Input motions

Pseudo acceleration spectra, time histories of acceleration and energy spectra are shown in Fig.11. Input motions were artificial earthquakes having an idealized response spectrum, and two types of phase characteristics were selected having long and short duration of primary wave: Hachinohe NS, the 1968 Tokachi earthquake and JMA Kobe NS, the 1995 Hyogoken-nambu earthquake. 100% of the intensity corresponds to very rare level of earthquake in the Japanese Building Standard Law. As shown in Fig.11, the two motions have similar response spectra with two different damping ratio(0.05 and 0.20), but the duration times of the primary waves are quite different.

The test procedure is as follows. 100% intensity of motions were applied ten times following 50% intensity of motion. If a specimen collapsed during an input motion, the additional weights were removed, and the other specimens were subjected to the next input motions. Firstly, the above procedure was conducted with Hachinohe wave. After that, all specimens were replaced by new ones, and the other procedure with Kobe wave was conducted. 150% intensity of motion was applied at the end only in the case of Kobe wave.

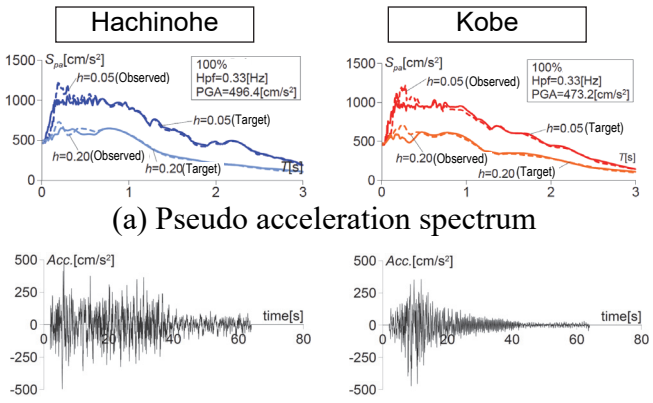

(a) Pseudo acceleration spectrum

(b) Time history

Fig.11 Characteristics of input motions

3.3 Test result

Maximum story drift angle in each input motion is shown in Fig.12. Hachinohe wave caused rapid increasing of story drift compared to Kobe wave, which was probably due to the long duration time and the large input energy. In the case of grade3, maximum drifts by Hachinohe and Kobe were close until a certain level of maximum drift, which is obvious by considering elastic response. However, if maximum drift angle exceeded around $1/3\delta_u$, the difference was rapidly made. Therefore, $1/3\delta_u$ can be a rough standard to prevent performance deterioration and to protect post-earthquake functional use.

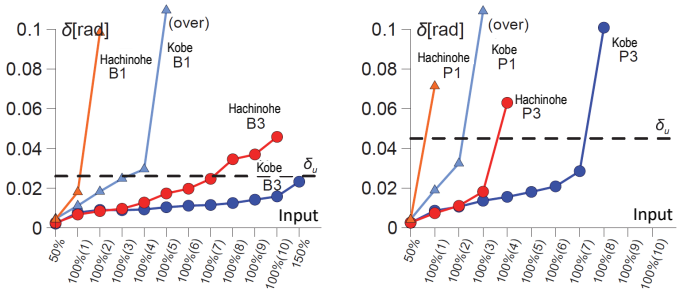

(a) Brace type (b) Plywood type

Fig.12 Maximum story drift angle

4. Evaluation of performance deterioration

4.1 Strength deterioration

Well-known cumulative damage rule, which predicts fatigue life of materials, is of practical use because cumulative damage by various levels of deformation can be expressed as a simple multiplication formula. Although fatigue failure has been observed in nail joints as shown in Fig.7 and Fig.8, it is difficult to define fatigue failure of shear walls. In this paper, a tendency of strength degradation is focused on, and the function of $f(\Delta, n)$ defined in section2.4 is extended to random loading as follows.

$$f(\Delta,n)=\left(1-f_\infty(\Delta)\right)\prod_{i=1}^{n}\left(\phi(\Delta,\Delta_i)e^{-\lambda(\Delta_i)}+1-\phi(\Delta,\Delta_i)\right)+f_\infty(\Delta) \quad (1)$$

Where, Π is a symbol of infinite product, $f_\infty(\Delta)$ is a convergent value of $f(\Delta, n)$ in $n\rightarrow\infty$, $\lambda(\Delta)$ is a rapidity of strength convergence and $\phi(\Delta, \Delta_i)$ is a reduction factor of damage in i-th cycle. Note that only expanded

cycles are counted as shown in Fig.3(d),(e)(white circular plots), and the corresponding amplitude ratio in *i*-th cycle is expressed as Δ_i.

The formula includes three parameters: $f_\infty(\Delta)$, $\lambda(\Delta)$ and $\phi(\Delta, \Delta_i)$. In constant amplitude loading at target amplitude Δ, $\phi(\Delta, \Delta_i) = 1$ can be assumed, and Eq.(1) can be rewritten by Eq.(2) as follows.

$$f(\Delta, n) = \left(1 - f_\infty(\Delta)\right) e^{-\lambda(\Delta) n} + f_\infty(\Delta) \tag{2}$$

The above equation satisfies "1" in $n = 0$ and "$f_\infty(\Delta)$" in $n = \infty$, respectively. The exponential function is capable of tracing the curves in Fig.5. $f_\infty(\Delta)$ and $\lambda(\Delta)$ can be obtained by least square method in each Δ.

As for $\phi(\Delta, \Delta_i)$, a damage sustained in small deformation results in "perfect restoration"($\phi(\Delta, \Delta_i) = 0$) while a damage in large deformation is close to "non restoration"($\phi(\Delta, \Delta_i) = 1$) as shown in Fig.4(b) and Fig.13. Restraint condition that $\phi(\Delta, \Delta_i) = 0$ in $\Delta_i = 0$ and $\phi(\Delta, \Delta_i) = 1$ in $\Delta_i = \Delta$ must be satisfied as well. As a result of numerical experiments, a power function like $\phi(\Delta, \Delta_i) = (\Delta_i/\Delta)^\alpha$ is thought to give better estimation. Using $f_\infty(\Delta)$ and $\lambda(\Delta)$ which have been already obtained, α is determined to fit the envelope curve to standard loading test for brace type and to long duration random loading test for plywood type. The tendencies of parameters and approximation functions(dash or solid lines) are shown in Fig.14.

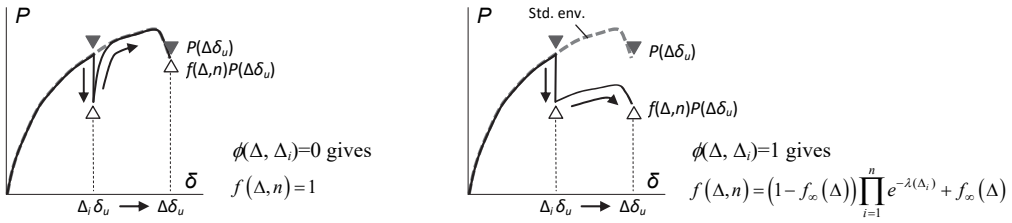

(a) Perfect restoration (b) Non restoration

Fig.13 Prameter controlling the effect of damage sustained in the past stage $\phi(\Delta, \Delta_i)$

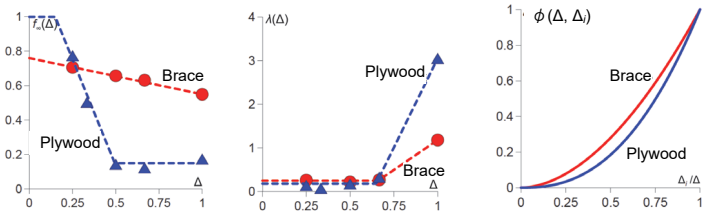

(a) $f_\infty(\Delta)$ (b) $\lambda(\Delta)$ (c) $\phi(\Delta, \Delta_i)$

For brace type:

$$f_\infty(\Delta) = -0.21\Delta + 0.76$$
$$\lambda(\Delta) = \begin{cases} 0.25 & (0 \le \Delta \le 0.66) \\ 2.74\Delta - 1.56 & (0.66 < \Delta \le 1) \end{cases}$$
$$\phi(\Delta, \Delta_i) = (\Delta_i/\Delta)^{1.84}$$

For plywood type:

$$f_\infty(\Delta) = \begin{cases} 1 & (0 \le \Delta < 0.15) \\ -2.47\Delta + 1.37 & (0.15 \le \Delta \le 0.49) \\ 0.15 & (0.49 < \Delta \le 1) \end{cases}$$
$$\lambda(\Delta) = \begin{cases} 0.18 & (0 \le \Delta < 0.65) \\ 8.17\Delta - 5.12 & (0.65 \le \Delta \le 1) \end{cases}$$
$$\phi(\Delta, \Delta_i) = (\Delta_i/\Delta)^{2.44}$$

Fig.14 Tendency of parameters and the approximation functions

A comparison between test results and estimated results is shown in Fig.15. As for the results of shaking table tests, the positive side was defined as the one having higher strength, and results of grade3 were omitted due to space limitation. Since envelope curves in shaking table tests were plotted upward rather than monotonic loading curves in static tests(standard envelope), force of the standard envelope is multiplied by a calibration factor. The factor is defined as the ratio of secant stiffness passing through points at 1/450rad and 1/300rad. The values ranging from 1.1 to 1.2 might have physical meanings derived from differences in loading velocity or boundary condition, but they are not a goal of this research. As shown in Fig.15, estimated results are likely to have acceptable accuracy.

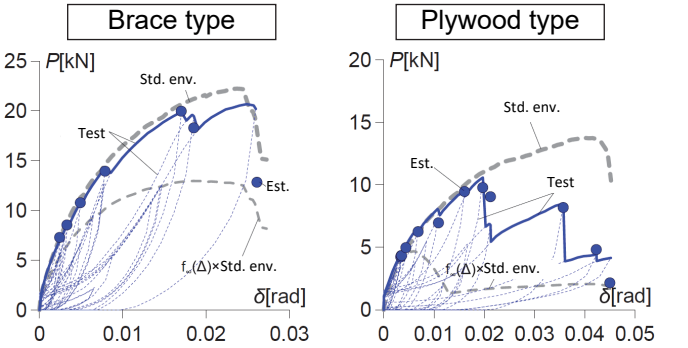

(a) Random loading(Long duration, Static)

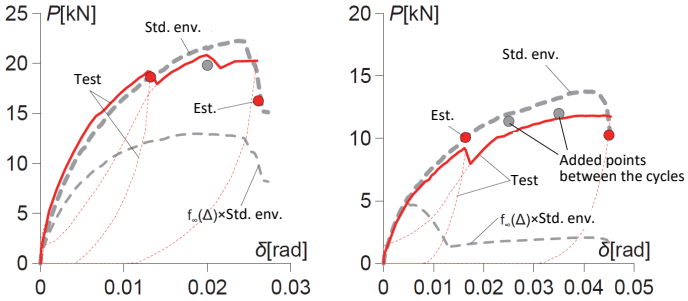

(b) Random loading(Short duration, Static)

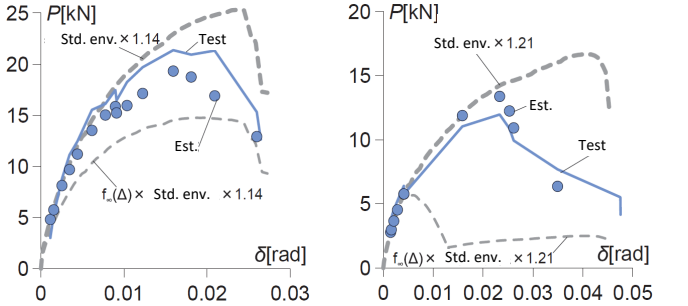

(c) Hachinohe (Grade1, Shaking table)

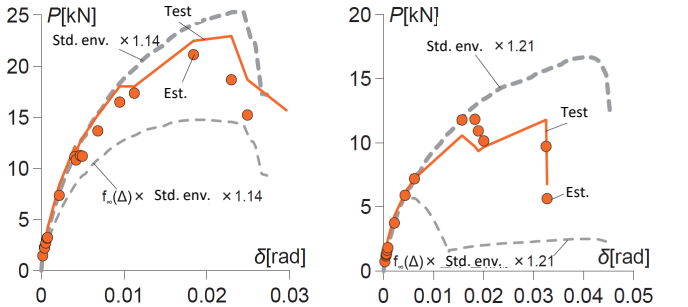

(d) Kobe (Grade1, Shaking table)

Fig.15 Prediction of force-deformation angle relation by proposed formula

4.2 Energy dissipation deterioration

Equivalent damping ratio h_{eq} is likely to be associated with maximum deformation which has been already experienced rather than the number of cycles. The tendency of h_{eq} can be summarized with respect to each Δ_n/Δ as shown in Fig.16. Where, Δ_n/Δ is maximum deformation which has been experienced so far normalized by target deformation. In this paper, $\Delta = 1$ is considered, which means damping ratio at ultimate deformation is focused on. Approximate equations are also illustrated in Fig.16 with black dash line.

It is found that the plots of random loading tests also follow the same trend. As stated above, h_{eq} is likely to be strongly correlated with Δ_n/Δ. The plots of shaking table tests, which are calculated using a cycle near ultimate deformation, seem to be a little higher than the others. It might be related to viscous damping due to dynamic loading, and the plo ts are nearly on the approximate lines plus 0.05(gray dash line).

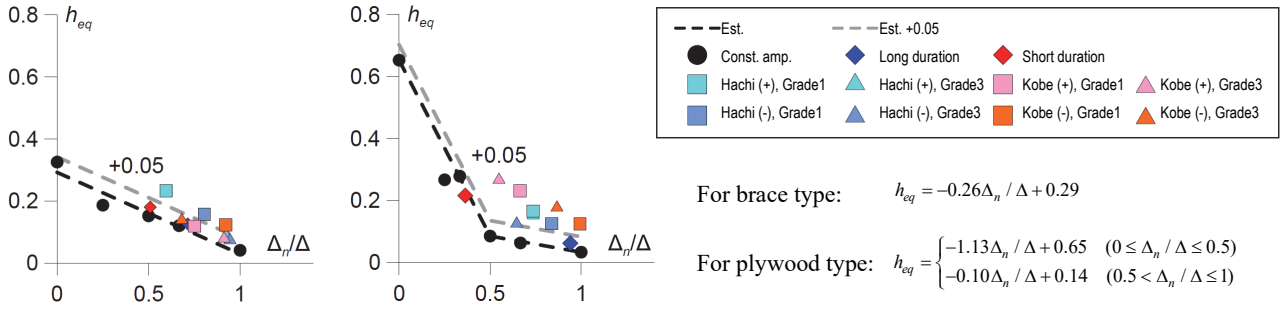

For brace type: $h_{eq} = -0.26\Delta_n/\Delta + 0.29$

For plywood type: $h_{eq} = \begin{cases} -1.13\Delta_n/\Delta + 0.65 & (0 \le \Delta_n/\Delta \le 0.5) \\ -0.10\Delta_n/\Delta + 0.14 & (0.5 < \Delta_n/\Delta \le 1) \end{cases}$

(a) Brace type (b) Plywood type

Fig.16 Equivalent damping ratio with respect to each experienced maximum deformation (Δ_n/Δ) and the approximation functions

5. Conclusions

In this paper, static cyclic loading tests and shaking table tests of wooden brace walls and plywood sheathing walls were conducted, and the deterioration of strength and energy dissipation was evaluated. The followings are findings of this paper.

1) Envelope curve of force-deformation angle relation has a dependency on loading protocol. The envelope curve in monotonic loading is the upper bound, and the others go downward as the number of cycles increases.

2) Plywood type shear walls are vulnerable to repeated loading rather than brace type shear walls, which is likely to be related to the failure mode. As for plywood type, failure mode of nail joints change from punching out to bending failure as the number of cycles increases.

3) When two earthquakes having the same response spectrum shape but different duration time were repeatedly applied, the one having longer duration time rapidly brought deformation increase. It is likely to be related to fatigue behavior owing to repeated loading.

4) Both brace type and plywood type specimens kept seismic performance against repeated earthquake motions if the maximum deformation response was less than one-third of the ultimate deformation.

5) Evaluation formulae for strength and equivalent damping ratio considering fatigue behavior were proposed. They showed acceptable agreement with the results of static random loading tests and shaking table tests.

Acknowledgements

The shaking table test was carried out using Large-scale Earthquake Simulator of National Research Institute for Earth Science and Disaster Resilience. This work was supported by JSPS KAKENHI Grant Number JP 17H04943. The authors would like to express special thanks to them.

References

[1] Japan Housing and Wood Technology Center (2017) : Allowable Strength Design for Post and Beam Wooden Houses, 2017.3

[2] Kazuhiko Kasai, Akira Wada, Mitsumasa Midorikawa, Hiroyasu Sakata and Yoji Ooki (2004) : Development of Passively-Controlled Wooden Houses with Superior Property-Retention Capability Part 1 Project Overview, *Summaries of Technical Papers of Annual Meeting*, Architectural Institute of Japan, B-2, pp.115-116, 2004.7

[3] Satori Nakanishi, Yoshihiro Yamazaki and Hiroyasu Sakata (2018) : Proposal of Performance Evaluation Method for Passively Controlled Timber Houses Subjected to Repeated Earthquakes, *Summaries of Technical Papers of Annual Meeting*, Architectural Institute of Japan, Structure III, pp.57-58, 2018.7

[4] Hiroki Minemura, Hiroshi Isoda and Manabu Hattori (2014) : Shaking Table Test of Wood House with No Degradation Shear Wall to Sustain Seismic Performance against Aftershock and Cyclic Loading, *Journal of Structural and Construction Engineering(Transactions of AIJ)*, 698, pp.491-498, 2014.4

[5] Bryan Folz and Andre Filiatrault (2001) : Cyclic Analysis of Wood Shear Walls, *Journal of Structural Engineering*, ASCE, 127(4), April 2001

[6] Weichiang Pang, D. V. Rosowsky, Shiling Pei and John W. van de Lindt (2007) : Evolutionary Parameter Hysteretic Model for Wood Shear Walls, *Journal of Structural Engineering*, ASCE, 133(8), August 2007

[7] Yusaku Hitomi, Hiroshi Isoda and Naohito Kawai (2009) : Hysteresis Model of Wood Shear Wall Considering of Large Displacement and Deterioration of Cyclic Load : Study on Seismic Behavior of Wooden Construction Part 2, *Journal of Structural and Construction Engineering(Transactions of AIJ)*, 646, pp.2299-2306, 2009.12

[8] Hiroshi Isoda, Yusaku Hitomi and Tatsuya Miyake (2010) : Derivation and Application of Limit State Curve Based on Maximum Displacement and Cumulative Energy for Wood Shear Wall, *Journal of Structural and Construction Engineering(Transactions of AIJ)*, 647, pp.185-192, 2010.1

[9] Hiroshi Isoda (2011) : Verification of Hysteresis Model of Wood Shear Wall Considering of Large Displacement under Earthquakes, *Journal of Structural and Construction Engineering(Transactions of AIJ)*, 659, pp.113-120, 2011.1

[10] Masashi Shiomitsu, Yuki Sakai, Hiroshi Isoda, Yasuhiro Araki and Taizo Matsumori (2018) : Development of Hysteresis Characteristics Model for Existing Wooden Houses, *Journal of Structural and Construction Engineering(Transactions of AIJ)*, 747, pp.717-726, 2018.5

[11] Yoshihiro Yamazaki, Kengo Kanda and Hiroyasu Sakata (2019) : Strength and Energy Dissipation of Timber Shear Walls Subjected to Arbitrary Deformation History: Study on Fatigue Behavior of Timber Structures Subjected to Repeated Earthquake Motions : part1, *Journal of Structural and Construction Engineering(Transactions of AIJ)*, 765, pp.1443-1451, 2019.11

